

# Simplified Projectile Swerve Solution for General Control Inputs

Douglas Ollerenshaw\*

Oregon State University, Corvallis, Oregon 97331

and

Mark Costello†

Georgia Institute of Technology, Atlanta, Georgia 30332

DOI: 10.2514/1.34252

The swerve response of fin- and spin-stabilized projectiles to control mechanism inputs is sometimes not intuitive. This paper seeks to explain the basic parameters that govern the swerve of projectiles excited by control inputs. By modeling the overall effect of a generalized control mechanism as a nonrolling reference frame force applied to a point on the projectile, general expressions for swerve are obtained in terms of basic vehicle parameters. These compact expressions are used to show that maximum swerve response for a fin-stabilized projectile is achieved when the force is applied near the nose of the projectile, whereas maximum swerve response for a spin-stabilized projectile is achieved when the force is applied near the base of the projectile.

## Nomenclature

$C_{MQ}$	= pitch damping aerodynamic coefficient
$C_{NA}$	= normal force aerodynamic coefficient
$C_{YPA}$	= Magnus force aerodynamic coefficient
$D$	= projectile reference diameter
$F_c$	= magnitude of the applied control force
$g$	= gravity
$I_P$	= pitch moment of inertia measured around an axis centered at the projectile center of mass and perpendicular to the axis of symmetry
$I_R$	= roll moment of inertia measured about the projectile axis of symmetry
$m$	= mass of the projectile
$p$	= projectile roll rate expressed in the body frame
$\tilde{q}, \tilde{r}$	= projectile pitch and yaw rates expressed in the no-roll frame
$R$	= magnitude of the swerve response
$s$	= dimensionless arc length
$\tilde{u}, \tilde{v}, \tilde{w}$	= projectile velocity components expressed in the no-roll frame
$V$	= total velocity
$x, y, z$	= projectile position in inertial space
$Y_c, Z_c$	= $y$ and $z$ components applied control force expressed in no-roll frame
$\Delta_{SLC}$	= station line distance from the projectile mass center to the point of application of the control force
$\Delta_{SLM}$	= station line distance from the projectile mass center to the point of application of the Magnus force
$\Delta_{SLP}$	= station line distance from the projectile mass center to the center of pressure
$\lambda_{FR}, \lambda_{FI}$	= real and imaginary parts of the fast-mode epicyclic eigenvalues
$\lambda_{SR}, \lambda_{SI}$	= real and imaginary parts of the slow-mode epicyclic eigenvalues

Received 27 August 2007; revision received 30 November 2007; accepted for publication 6 December 2007. Copyright © 2007 by the American Institute of Aeronautics and Astronautics, Inc. All rights reserved. Copies of this paper may be made for personal or internal use, on condition that the copier pay the \$10.00 per-copy fee to the Copyright Clearance Center, Inc., 222 Rosewood Drive, Danvers, MA 01923; include the code 0731-5090/08 \$10.00 in correspondence with the CCC.

\*Department of Mechanical Engineering; currently Consulting Engineer, Earthly Dynamics LLC, Atlanta, GA 30327.

†Sikorsky Associate Professor, School of Aerospace Engineering. Associate Fellow AIAA.

$\rho$	= atmospheric density
$\Phi_R$	= phase shift of the swerve response
$\phi, \theta, \psi$	= projectile roll, pitch, and yaw angles
$\sim$	= denotes variables expressed in the projectile no-roll frame
$'$	= prime denotes variables differentiated with respect to dimensionless arc length

## I. Introduction

THE continuing development of microelectromechanical systems (MEMS) is pointing to the possibility of mounting complete sensor systems on medium- and small-caliber projectiles as part of an actively controlled smart munition. Two important technical challenges in achieving this goal are the development of small, rugged, sensor suites and control mechanisms. There is currently a flurry of activity to create innovative physical control mechanisms. Concepts include pulse jets, squibs, synthetic jets [1–3], drag brakes [4,5], deployable pins [6,7], moveable nose [8], moveable canards [9], dual-spin projectiles [10,11], ram air deflection [12], and internal translating mass [13], to name a few.

Although the preceding physical control mechanisms are very diverse, there is a common theme between them all: each exerts a force and/or moment on the projectile. Moreover, because trajectories are shaped relative to ground coordinates, the forces and moments are effectively applied in a nonrolling reference frame and can often be modeled as constant point forces applied to the projectile body. Although the uncontrolled dynamics of projectiles (both fin-stabilized and spin-stabilized) have been extensively studied in the ballistics community, issues with regard to control response have received considerably less attention due to the lack of practical application of control technology to spinning projectiles. Using projectile linear theory, this paper analytically investigates several aspects of the response of a spinning projectile to a constant control force in the nonrolling reference frame. Simple expressions result for the swerve-response magnitude and phase angle in terms of basic physical mass properties, aerodynamic characteristics, and the state of the air vehicle. These expressions provide a means toward deeper understanding of the underlying factors driving the control response of projectiles, helping smart-weapon designers to create more capable weapon systems.

## II. Simplified Analytical Swerve Solution

A six-degree-of-freedom (6-DOF) rigid-body dynamic model used to simulate the trajectory of a projectile in atmospheric flight is

well known [14]. Over time, however, a series of simplifications to the dynamic equations have been identified that result in an analytically solvable set of quasi-linear differential equations and reasonably accurate trajectories. These equations are referred to collectively as projectile linear theory [15]. The linear theory dynamic equations that are applicable to this analysis are given as Eqs. (1–6):

$$\begin{Bmatrix} \tilde{v}' \\ \tilde{w}' \\ \tilde{q}' \\ \tilde{r}' \end{Bmatrix} = \begin{bmatrix} -A & 0 & 0 & -D \\ 0 & -A & D & 0 \\ \frac{B}{D} & \frac{C}{D} & H & -F \\ -\frac{C}{D} & \frac{B}{D} & F & H \end{bmatrix} \begin{Bmatrix} \tilde{v} \\ \tilde{w} \\ \tilde{q} \\ \tilde{r} \end{Bmatrix} + \begin{Bmatrix} V_F \\ W_F \\ Q_F \\ R_F \end{Bmatrix} \quad (1)$$

$$\theta' = \frac{D}{V} \tilde{q} \quad (2)$$

$$\psi' = \frac{D}{V} \tilde{r} \quad (3)$$

$$x' = D \quad (4)$$

$$y' = \frac{D}{V} \tilde{v} + \psi D \quad (5)$$

$$z' = \frac{D}{V} \tilde{w} - \theta D \quad (6)$$

The projectile linear theory dynamic equations use dimensionless arc length  $s$  as the independent variable. Arc length is related to time, as shown in Eq. (7):

$$s = \frac{1}{D} \int_0^t V dt \quad (7)$$

The prime notation employed in Eqs. (1–6) signifies that the derivatives are taken with respect to dimensionless arc length, as opposed to time. Additionally, the linear theory equations employ a reference frame that is aligned with the projectile axis of symmetry but does not roll. Variables in this reference frame, which is referred to as the no-roll frame or the fixed plane frame, are denoted with a tilde superscript. The no-roll frame is related to the body-fixed frame used in the traditional 6-DOF equations by a single axis rotation about the projectile axis of symmetry.

For the purpose of examining basic swerve response due to control inputs, both gravity and atmospheric winds are neglected. The constant terms in the set of four coupled equations shown as Eq. (1), referred to as the epicyclic equations, can then be described as

$$A = \frac{\pi \rho D^3 C_{NA}}{8m} \quad (8)$$

$$B = \frac{\pi \rho D^5 C_{YPA} p \Delta_{SLM}}{16I_p V} \quad (9)$$

$$C = \frac{\pi \rho D^4 C_{NA} \Delta_{SLP}}{8I_p} \quad (10)$$

$$F = \frac{I_R D p}{I_p V} \quad (11)$$

$$H = \frac{\pi \rho D^5 C_{MQ}}{16I_p} \quad (12)$$

$$V_F = \frac{DY_C}{mV} \quad (13)$$

$$W_F = \frac{DZ_C}{mV} \quad (14)$$

$$Q_F = -\frac{D \Delta_{SLC} Z_C}{I_p V} \quad (15)$$

$$R_F = \frac{D \Delta_{SLC} Y_C}{I_p V} \quad (16)$$

Both the velocity  $V$  and the roll rate  $p$  are considered to be constant in Eqs. (2–6) and (8–16).

The aerodynamic coefficients appearing in Eqs. (8–16) are defined as follows [16]. The term  $C_{NA}$  is the normal force coefficient. The normal force acts in a direction perpendicular to the projectile axis of symmetry and results from nonaxial wind forces caused by yawing and pitching of the projectile. The normal force does not act at the projectile center of gravity (c.g.), but at a point called the normal force center of pressure (COP). The  $\Delta_{SLP}$  term represents the distance between the center of gravity and the center of pressure, as shown in Eq. (17):

$$\Delta_{SLP} = SL_{COP} - SL_{c.g.} \quad (17)$$

where both the center of gravity and the center of pressure are measured from the projectile base along the projectile station line.  $C_{YPA}$  is the Magnus force coefficient. The Magnus force is perpendicular to the normal force and is caused by unequal pressures on opposite sides of the projectile resulting from viscous interaction between the spinning surface and the surrounding atmosphere. The Magnus force itself is generally considered to be small enough to be neglected; however, the resulting moment must be considered. The distance between the c.g. and the point of application of the Magnus force (Mag) is denoted as  $\Delta_{SLM}$ :

$$\Delta_{SLM} = SL_{Mag} - SL_{c.g.} \quad (18)$$

where both the center of gravity and the Magnus force application point are measured from the projectile base along the projectile station line. The Magnus force is proportional to both spin rate and transverse angular velocity. Therefore, in projectiles with very low spin rates, the Magnus moment approaches zero. The term  $C_{MQ}$  represents the pitch-damping-moment coefficient. The pitch damping moment is proportional to the transverse angular velocity of the projectile.  $C_{MQ}$  will always be negative for a stable projectile. Thus, it has the stabilizing effect of decreasing the total transverse angular velocity of the projectile.

Finally, the terms  $Y_C$  and  $Z_C$  represent the  $y$  and  $z$  components of a constant control force expressed in the no-roll frame and are assumed to act at a single point on the projectile with a moment arm  $\Delta_{SLC}$  defined as

$$\Delta_{SLC} = SL_{CF} - SL_{c.g.} \quad (19)$$

where both the center of mass and the point of application of the control force are measured from the rear of the projectile along the projectile axis of symmetry.

To arrive at expressions for swerve  $(y, z)$ , the solutions to the coupled epicyclic equations (5) must first be obtained. In the interest of brevity, this lengthy but mathematically conventional solution was omitted here. Substituting the solutions for  $\tilde{q}$  and  $\tilde{r}$  into the attitude equations  $(\theta, \psi)$ , then substituting the resulting attitude expressions, along with the solutions for  $\tilde{v}$  and  $\tilde{w}$ , into the swerve expressions results in the following expressions for

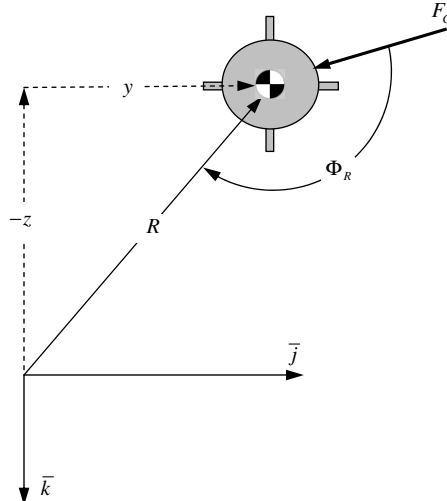


Fig. 1 Rear view of the projectile, showing position coordinate definitions. The positive  $\bar{i}$  and  $x$  directions point into the page.

projectile swerve:

$$\begin{aligned} y(s) = & C_{y0} + C_{y1}s + C_{y2}s^2 + e^{\lambda_{FR}s} (C_{yfc} \cos(\lambda_{FI}s) \\ & + C_{yfs} \sin(\lambda_{FI}s)) + e^{\lambda_{SR}s} (C_{ysc} \cos(\lambda_{SI}s) + C_{yss} \sin(\lambda_{SI}s)) \end{aligned} \quad (20)$$

$$\begin{aligned} z(s) = & C_{z0} + C_{z1}s + C_{z2}s^2 + e^{\lambda_{FR}s} (C_{zfc} \cos(\lambda_{FI}s) \\ & + C_{zfs} \sin(\lambda_{FI}s)) + e^{\lambda_{SR}s} (C_{zsc} \cos(\lambda_{SI}s) + C_{zss} \sin(\lambda_{SI}s)) \end{aligned} \quad (21)$$

The  $C$  terms in Eqs. (20) and (21) are constants containing projectile parameters, initial conditions, and input forces. Additionally, the downrange position of the projectile is simply

$$x(s) = x_0 + Ds \quad (22)$$

Equations (20–22) are expressed as a function of dimensionless arc length  $s$ , as defined in Eq. (7).

To obtain a sense of the generalized swerve response of a projectile due to an applied control force, we will examine the case in which the projectile is fired downrange with no initial pitch or yaw angle and with no initial perturbations to the transverse lateral and angular velocities. Assuming that the firing position is at the origin of the inertial reference frame, this allows us to set the initial conditions of all terms to zero, with the exception of velocity and roll rate. The velocity and roll-rate initial conditions are denoted  $V_0$  and  $p_0$ . Additionally, as stated earlier, the effects of both gravity and atmospheric winds are neglected here. These assumptions provide a case in which a projectile with no applied control force displays no swerving motion. Subsequently, the swerve response created by the application of a control force is clear.

Examining the swerve expressions in Eqs. (20) and (21), a few simplifications can be made. First of all, it should be noted that in a stable projectile, the real parts of the fast- and slow-mode eigenvalues,  $\lambda_{FR}$  and  $\lambda_{SR}$ , are always negative. Therefore, the oscillatory terms in the swerve-response decay as the projectile flies downrange and can be neglected for long-term swerve response. The pitch damping moment is primarily associated with the oscillatory epicyclic terms and can also be neglected, allowing  $C_{MQ}$  in Eq. (12) to be set to zero. Additionally, as the arc length value becomes large, the terms containing the square of the arc length begin to dominate the swerve-response expressions, and the terms involving  $C_{y0}$ ,  $C_{y1}$ ,  $C_{z0}$ , and  $C_{z1}$  can be neglected. These simplifications leave only the terms involving  $s^2$  in Eqs. (20) and (21). Finally, Eq. (22) can be solved for arc length  $s$  and substituted into Eqs. (20) and (21).

Table 1 Summary of the projectile initial conditions, physical parameters, and aerodynamic coefficients

	120-mm fin-stabilized projectile	155-mm spin-stabilized projectile
$V_0$ , ft/s	5479.0	2710.0
$p_0$ , rad/s	8.7000	1674.1
$\rho$ , slug/ft <sup>3</sup>	$2.3785 \times 10^{-3}$	$2.3785 \times 10^{-3}$
$I_R$ , slug · ft <sup>2</sup>	$2.3870 \times 10^{-4}$	0.10857
$I_P$ , slug · ft <sup>2</sup>	0.17718	1.3964
$m$ , slug	0.34461	2.9465
$D$ , ft	0.08790	0.50853
$C_{NA}$	13.350	2.6314
$C_{YPA}$	0.0000	-0.9600
$C_{MQ}$	-5215.8	-27.700
$SL_{c.g.}$ , ft	1.3833	1.0627
$\Delta_{SLM}$ , ft	0.0000	-0.52920
$\Delta_{SLP}$ , ft	-0.50079	0.71373

The resulting simplified swerve expressions are then functions of range solely in terms of projectile parameters, initial velocity and spin rate, and a control force applied in the no-roll frame. The equations for  $y$  and  $z$  can then be combined to create an expression for the overall magnitude of the swerve response. A compact and informative expression for the response magnitude  $R$  results:

$$R = \frac{F_C x^2}{2V_0^2} \sqrt{\frac{D^2 p_0^2 C_{YPA}^2 \Delta_{SLM}^2 + 4V_0^2 C_{NA}^2 (\Delta_{SLC} - \Delta_{SLP})^2}{p_0^2 (2I_R C_{NA} + mDC_{YPA} \Delta_{SLM})^2 + 4m^2 V_0^2 C_{NA}^2 \Delta_{SLP}^2}} \quad (23)$$

where  $F_C$  is the magnitude of the control force, defined as

$$F_C = \sqrt{Y_C^2 + Z_C^2} \quad (24)$$

The phase shift of the response,  $\Phi_R$ , is the angle between the direction of the applied control force and the direction of the response, as shown in Fig. 1. The phase shift can be expressed as

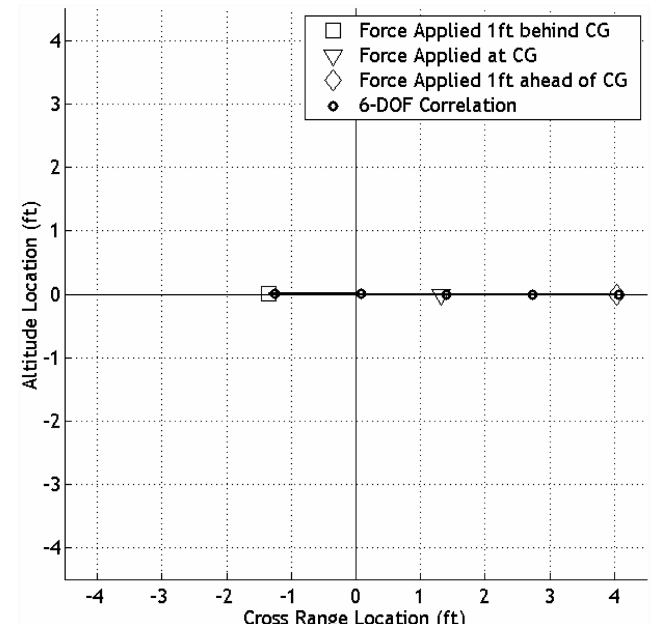


Fig. 2 Vertical plane swerve response of the fin-stabilized projectile at a range of 5280 ft to a 1-lbf control input applied in the  $+y$  direction, with 6-DOF correlation data.

$$\Phi_R = \tan^{-1} \left( \frac{2V_0 p_0 C_{NA} (2I_R C_{NA} (\Delta_{SLC} - \Delta_{SLP}) + mDC_{YPA} \Delta_{SLM} \Delta_{SLC})}{Dp_0^2 C_{YPA} \Delta_{SLM} (2I_R C_{NA} + mDC_{YPA} \Delta_{SLM}) - 4mV_0^2 C_{NA}^2 \Delta_{SLP} (\Delta_{SLC} - \Delta_{SLP})} \right) \quad (25)$$

The preceding equations provide relatively compact expressions for the swerve magnitude and phase shift resulting from a constant control force applied to a point on the projectile. These expressions highlight the key parameters that drive the control response of projectiles excited by a control-force input. However, when applying these formulas, it is important to recall that stability of the projectile is inherent in the assumptions used to arrive at the preceding expressions. When parameters are varied in these expressions to investigate the effects on swerve response, care must be taken to

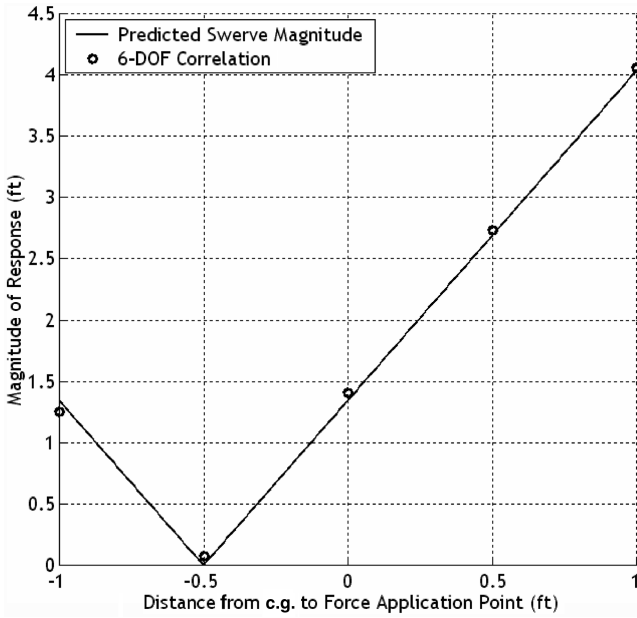


Fig. 3 Magnitude of the swerve response of the fin-stabilized projectile to a 1-lbf control input as a function of the distance from the projectile c.g. to the point of application of the force, with 6-DOF correlation data.

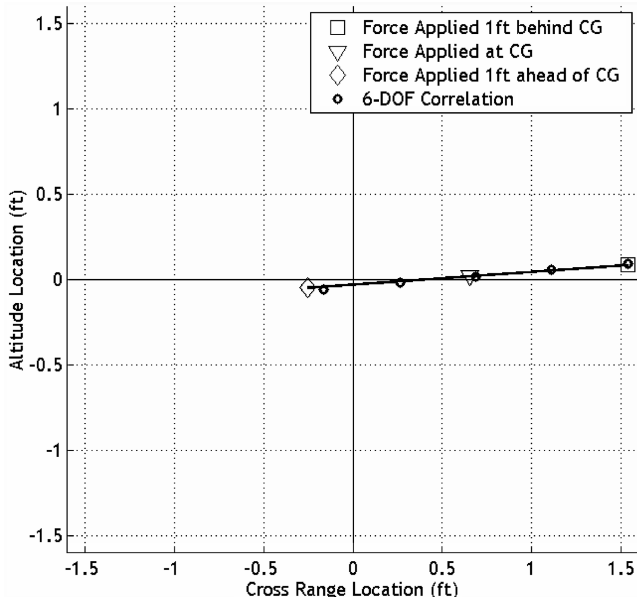


Fig. 4 Vertical plane swerve response of the spin-stabilized projectile at a range of 5280 ft to a 1-lbf control input applied in the +y direction, with 6-DOF correlation data.

ensure that the stability assumption is not violated. It also needs to be emphasized that these equations calculate the magnitude and phase shift of the swerve response under the assumption that the velocity and spin rate remain constant at their initial values and, in turn, all Mach-number-dependent quantities remain constant as well. Of

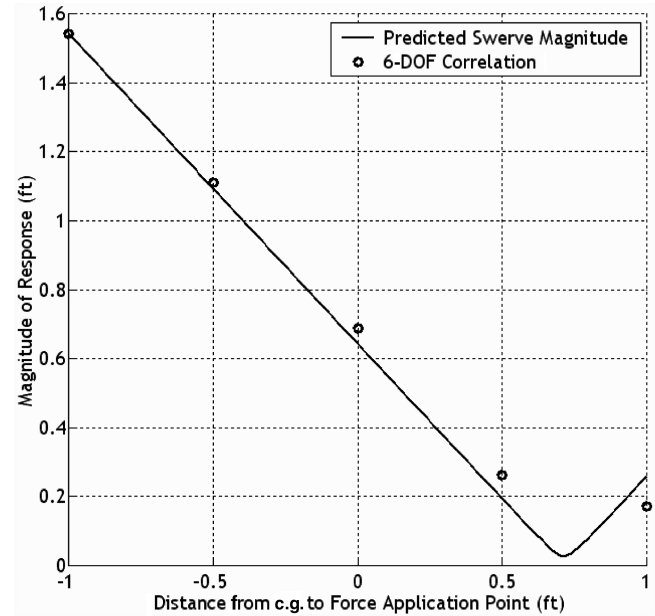


Fig. 5 Magnitude of the swerve response of the spin-stabilized projectile to a 1-lbf control input as a function of the distance from the projectile c.g. to the point of application of the force, with 6-DOF correlation data.

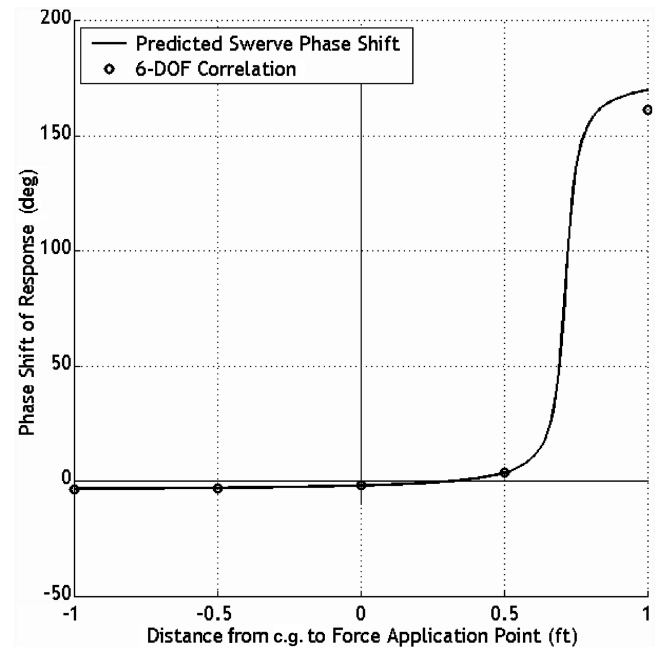


Fig. 6 Phase shift of the swerve response of the spin-stabilized projectile to a 1-lbf control input as a function of the distance from the projectile c.g. to the point of application of the force, with 6-DOF correlation data.

course, this assumption becomes increasingly inaccurate as the projectile proceeds downrange and must be periodically updated for long-range trajectories.

### III. Correlation to the Full Six-Degree-of-Freedom Model

To demonstrate the accuracy of the simplified swerve equations, a typical 120-mm fin-stabilized projectile and a typical 155-mm spin-stabilized projectile were evaluated. For both projectiles, the results obtained using Eqs. (23) and (25) were compared with results from a fixed-step, fourth-order Runge–Kutta numerical integration of the full 6-DOF equations of motion. The swerve response was evaluated at a range of 5280 ft in the absence of gravity and atmospheric winds and with no initial yaw or pitch angles. In both cases, a 1-lbf control input was applied in the positive  $y$  direction. The control-force moment arm  $\Delta_{SLC}$  in Eqs. (23) and (25) was varied from 1 ft behind the projectile center of mass to 1 ft in front of the projectile center of mass. The 6-DOF swerve response was evaluated for both projectiles with control-force moment arms of  $\Delta_{SLC} = -1.0, -0.5, 0.0, 0.5$ , and 1.0 ft.

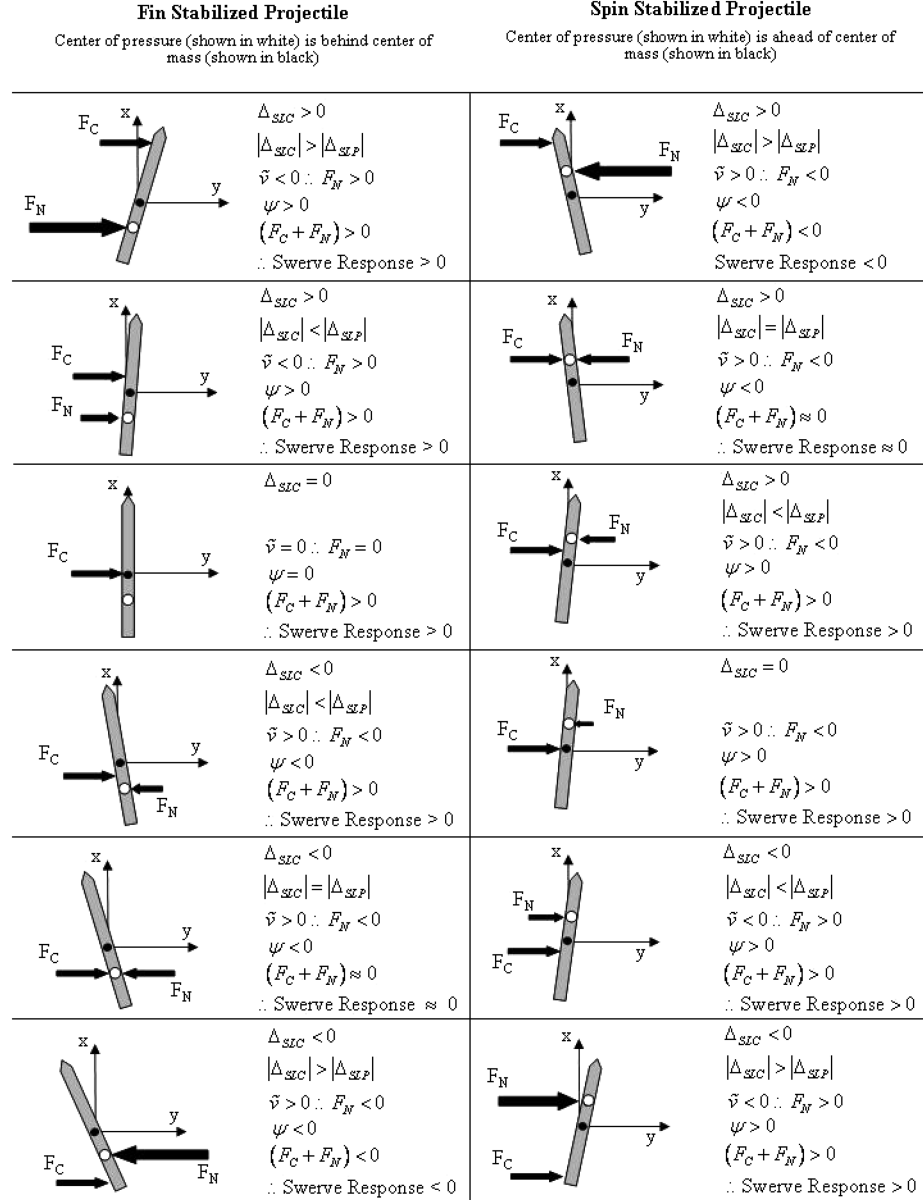


Fig. 7 Summary of the projectile response to a control input in the positive  $y$  direction in both a fin-stabilized and a spin-stabilized projectile. Magnus moments, which act 90 deg out of phase with the angle of attack in spin-stabilized projectiles, are not shown.

Table 1 summarizes the initial conditions and the resultant aerodynamic coefficients, along with the relevant physical parameters, for both projectiles, as used in Eqs. (23) and (25).

Figure 2 shows the swerve response of the fin-stabilized projectile in the vertical target plane at a downrange location of  $x = 5280$  ft, with five 6-DOF data points included to demonstrate correlation. It should be noted that the positive  $z$  direction points downward, in the negative altitude direction. Figure 3 shows the magnitude of the response as a function of control-force application point, along with 6-DOF correlation data for the fin-stabilized projectile. Note that the magnitude of the response is dependent only upon the magnitude of the control input, not its direction. The phase shift, which is simply 0 deg when the force is applied in front of the COP and 180 deg when it is applied behind the COP, is not shown. The phase shift of the response does not vary with the magnitude of the input and is also independent of the direction of the input force.

Figure 4 shows the swerve response of the spin-stabilized projectile in the vertical target plane at a downrange location of  $x = 5280$  ft, with five 6-DOF data points included to demonstrate correlation. Figures 5 and 6 show the magnitude and phase shift of the response along with 6-DOF correlation data for the spin-stabilized projectile.

For both the fin-stabilized and spin-stabilized projectiles studied here, the response as predicted by the simplified swerve equations is shown to correlate very well with that predicted by the full 6-DOF simulation at this relatively short range. Though only a very small fraction of the total terms comprising the full linear theory swerve expressions are preserved in the simplified version, it is clear that those terms providing the dominant effect on the swerve response have been retained.

#### IV. Effects of Individual Parameters

Figures 2–6 clearly show that the point of application of the control force has a very large effect on both the direction and the magnitude of the swerve response. Further, they demonstrate that the effects are drastically different for fin- and spin-stabilized projectiles. The simplified swerve expressions provide insight into the reasons for this behavior. In the swerve-response magnitude and phase expressions given as Eqs. (23) and (25), the term expressing the distance from the center-of-pressure location to the point of application of the control force ( $\Delta_{SLC} - \Delta_{SLP}$ ) shows up repeatedly. The practical result is that if the control force is applied at the center of pressure,  $\Delta_{SLC} - \Delta_{SLP}$  becomes zero and the response magnitude is at a minimum. In the case of a fin-stabilized projectile, which has very low spin rates and negligibly small Magnus effects as a result, the magnitude of the response goes to zero when the control force is applied at the center of pressure.

The direction of the response is also driven by the center-of-pressure location relative to the projectile mass center. A typical fin-stabilized projectile will have a center-of-pressure location behind the projectile center of mass. A control force applied in front of the center of pressure leads to a response largely in phase with the direction of the control force. Conversely, when the control force is applied behind the center of pressure, the response is nearly 180 deg out of phase with the direction of the control force.

A spin-stabilized projectile, which typically has its center of pressure located in front of the center of mass, displays the opposite behavior. Additionally, the Magnus moment causes a relatively small response that is 90 deg out of phase with the direction of the applied control force.

The physical explanation for this behavior is relatively straightforward. Application of a control force away from the center of gravity creates a nonzero angle of attack in the projectile. The normal force results directly from the angle of attack, and in a stable projectile, it will create a moment equal and opposite to the moment caused by the control input after the initial oscillatory epicyclic dynamics decay, creating a zero net moment on the body. The direction of the response will be driven primarily by the sum of these two forces. When the control force is applied at the center of pressure, the normal force will be equal and opposite to the control force and the response will be driven solely by the Magnus effect, which has a nonnegligible effect only in spin-stabilized projectiles. Figure 7 graphically summarizes the effects of a control force in the positive  $y$  direction applied at varying points on the projectile body.

To demonstrate the relatively small contribution of the Magnus moment in a spin-stabilized projectile, the swerve magnitude and phase shift of the spin-stabilized projectile were examined with the Magnus force coefficient equal to the nominal value ( $-0.96$ ), half the nominal value ( $-0.48$ ), and zero.

The magnitude of the response is largely unaffected by reducing or removing the Magnus moment, with the exception being when the control force is applied near the projectile center of pressure. When that is the case, the sum of the normal force and control force nears zero and the Magnus moment becomes the dominant factor in the response magnitude. When the Magnus moment is neglected entirely, the magnitude of the response of the spin-stabilized projectile becomes zero when the control force is applied at the center of pressure, as is the case in a fin-stabilized projectile.

The effect of the Magnus moment becomes more apparent when examining the phase response of the spin-stabilized projectile with varied Magnus force coefficients, as shown in Fig. 8. The Magnus moment acts 90 deg out of phase with the angle of attack of the

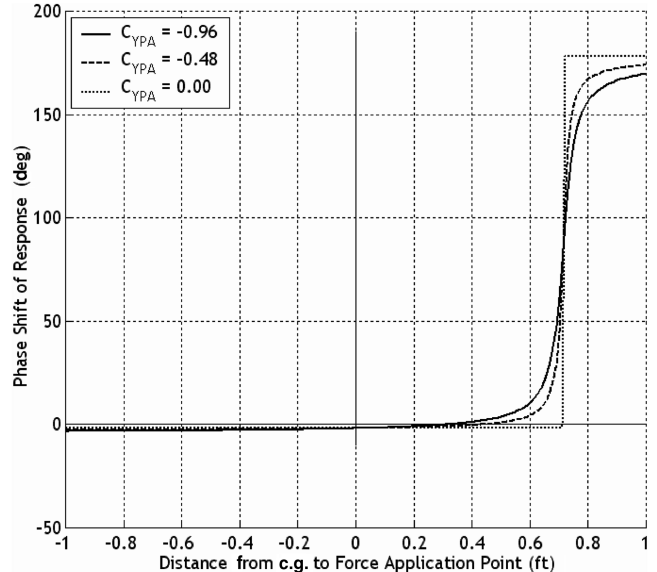


Fig. 8 Phase shift of the swerve response of the spin-stabilized projectile to a 1-lbf control input as a function of the distance from the projectile c.g. to the point of application of the control force. Magnus force coefficient is varied from its nominal value to zero.

projectile. As the Magnus force coefficient is reduced, the portion of the response that is orthogonal to the control input diminishes. With no Magnus moment present, the response is almost completely in phase with a force applied behind the center of pressure and is nearly 180 deg out of phase for a force applied in front of the center of pressure.

#### V. Conclusions

Relatively simple, closed-form formulas for the magnitude and phase angle of a projectile excited by a control force in terms of fundamental projectile flight mechanic parameters were created. The swerve-response formulas are remarkably accurate given the litany of simplifications and the resulting compact form of the results. These formulas clearly explain the control response differences between fin- and spin-stabilized projectiles, including the key role that the center of pressure plays in control-force response. It is shown that fin-stabilized projectiles respond in phase to control-force inputs forward of the center of pressure whereas spin-stabilized projectiles respond out of phase to control-force inputs forward of the center of pressure. The simple formulas reported here are expected to be useful to smart-weapon designers in bringing to light basic parameters that drive swerve response from different control mechanisms.

#### References

- [1] Harkins, T., and Brown, T., "Using Active Damping as a Precision-Enhancing Technology for 2.75-Inch Rockets," U. S. Army Research Lab., ARL-TR-1772, Aberdeen Proving Ground, MD, 1999.
- [2] Jitraphai, T., and Costello, M., "Dispersion Reduction of a Direct Fire Rocket Using Lateral Pulse Jets," *Journal of Spacecraft and Rockets*, Vol. 38, No. 6, 2001, pp. 929–936.
- [3] Amitay, M., Smith, D., Kibens, V., Parekh, D., and Glezer, A., "Aerodynamic Flow Control over an Unconventional Airfoil Using Synthetic Jet Actuators," *AIAA Journal*, Vol. 39, No. 3, 2001, pp. 361–370.
- [4] Harkins, T., and Davis, B., "Drag-Brake Deployment Method and Apparatus for Range Error Correction of Spinning, Gun-Launched Artillery Projectiles," U.S. Patent 6345785, issued 12 Feb. 2002.
- [5] Hillstrom, T., and Osborne, P., "United Defense Course Correcting Fuze for the Precision Guidance Kit Program," *49th Annual Fuze Conference*, National Defense Industrial Association, Arlington, VA, 5–7 Apr. 2005, [http://proceedings.ndia.org/5560/Wednesday/Session\\_III-A/Osborne.pdf](http://proceedings.ndia.org/5560/Wednesday/Session_III-A/Osborne.pdf).
- [6] Massey, K., and Flick, A., "Mechanical and Jet Actuators for Guiding a

- Small Caliber Subsonic Projectile," 25th AIAA Applied Aerodynamics Conference, Miami, FL, AIAA Paper 2007-3813, 25–28 June 2007.
- [7] Massey, K., McMichael, J., Warnock, T., and Hay, F., "Mechanical Actuators for Guidance of a Supersonic Projectile," 23rd AIAA Applied Aerodynamics Conference, Toronto, Ontario, Canada, AIAA Paper 2005-4970, 6–9 June 2005.
- [8] Costello, M., and Agarwalla, R., "Improved Dispersion of a Fin Stabilized Projectile Using a Passive Moveable Nose," *Journal of Guidance, Control, and Dynamics*, Vol 23, No. 5, 2000, pp 900–903; also Errata, Vol. 25, No. 2, 2002, pp. 414.
- [9] Costello, M., "Extended Range of a Gun Launched Smart Projectile Using Controllable Canards," *Shock and Vibration*, Vol 8, Nos. 3–4, 2001, pp. 203–213.
- [10] Costello, M., and Peterson, A., "Linear Theory of a Dual Spin Projectile in Atmospheric Flight," *Journal of Guidance, Control, and Dynamics*, Vol. 23, No. 5, 2000, pp. 789–797.
- [11] Burchett, B., Peterson, A., and Costello, M., "Prediction of Swerving Motion of a Dual-Spin Projectile with Lateral Pulse Jets in Atmospheric Flight," *Mathematical and Computer Modelling*, Vol. 35, No. 7–8, 2002, pp. 821–834.  
doi:10.1016/S0895-7177(02)00053-5
- [12] Chandgadkar, S., Costello, M., Dano, B., Liburdy, J., and Pence, D., "Performance of a Smart Direct Fire Projectile Using a Ram Air Control Mechanism," *Journal of Dynamic Systems, Measurement, and Control*, Vol. 124, No. 4, 2002, pp. 606–612.  
doi:10.1115/1.1514666
- [13] Rogers, J., and Costello, M., "Control Authority of a Projectile Equipped with an Internal Translating Mass," 2007 AIAA Atmospheric Flight Mechanics Conference, Hilton Head, SC, AIAA Paper 2007-6492, 2007.
- [14] McCoy, R. L., "Six-Degrees-of-Freedom (6 DOF) and Modified Point-Mass Trajectories," *Modern Exterior Ballistics: the Launch and Flight Dynamics of Symmetric Projectiles*, Schiffer Publishing, Atglen, PA, 1999, pp. 187–212.
- [15] Hainz, L., and Costello, M., "Modified Projectile Linear Theory for Rapid Trajectory Prediction," *Journal of Guidance, Control, and Dynamics*, Vol. 28, No. 5, 2005, pp. 1006–1014.
- [16] McCoy, R. L., "Aerodynamic Forces and Moments Acting on Projectiles," *Modern Exterior Ballistics: the Launch and Flight Dynamics of Symmetric Projectiles*, Schiffer Publishing, Atglen, PA, 1999, pp. 32–40.